MiSer: An Optimal Low-Energy Transmission Strategy for IEEE 802.11a/h *

Daji Qiao+ Sunghyun Choi* Amit Jain+ Kang G. Shin+
+The University of Michigan
Ann Arbor, MI 48109, USA
{dqiao, amitj, kgshin}@eecs.umich.edu

*Seoul National University
Seoul, 151-744, Korea
schoi@snu.ac.kr

Abstract

Reducing the energy consumption by wireless communication devices is perhaps the most important issue in the widely-deployed and exponentially-growing IEEE 802.11 Wireless LANs (WLANs). TPC (Transmit Power Control) and PHY (physical layer) rate adaptation have been recognized as two most effective ways to achieve this goal. The emerging 802.11h standard, which is an extension to the current 802.11 MAC and the high-speed 802.11a PHY, will provide a structured means to support intelligent TPC.

In this paper, we propose a novel scheme, called *MiSer*, that minimizes the communication energy consumption in 802.11a/h systems by combining TPC with PHY rate adaptation. The key idea is to compute offline an optimal rate-power combination table, and then at runtime, a wireless station determines the most energy-efficient transmission strategy for *each* data frame by a simple table lookup. Another key contribution of this paper is to provide a rigorous analysis of the relation among different radio ranges and TPC's effect on the interference in 802.11a/h systems, which justifies MiSer's approach to ameliorating the TPC-caused interference by transmitting the CTS frames at a stronger power level. Our simulation results show that MiSer delivers about 20% more data per unit of energy consumption than the PHY rate adaptation scheme without TPC, while outperforming single-rate TPC schemes significantly thanks to the excellent energy-saving capability of PHY rate adaptation.

Categories and Subject Descriptors

C.2.1 [**Network Architecture and Design**]: Wireless Communication

General Terms

Algorithms, Design, Performance

*The work reported in this paper was supported in part by AFOSR under Grant No. F49620-00-1-0327 and DARPA under US AFRL Contract F30602-01-02-0527.

MobiCom'03, September 14–19, 2003, San Diego, California, USA.

Keywords

IEEE 802.11a/h, MiSer, TPC, PHY Rate Adaptation

1. Introduction

Most wireless stations, such as laptops and palmtops, are battery-powered and hence have a limited amount of energy. It is, therefore, very important to reduce the energy consumption by wireless communication devices. Our main goal in this paper is to achieve the energy-efficient data communication in the IEEE 802.11 WLANs (Wireless Local-Area Networks), or more specifically, the emerging 802.11a/h systems.

A WLAN device can be in one of the following modes: *transmit mode*, *receive mode*, *idle mode*, or *doze mode*. It consumes the highest power in the transmit mode and very little energy in the doze mode. In the idle mode, a WLAN device is required to sense the medium, and hence, consumes a similar amount of power as when it is in the receive mode [31]. Several power-management policies [20, 30, 31] have been proposed to force a WLAN device to enter the doze mode adaptively at appropriate moments to save battery energy.

An alternative way to conserve energy is to apply TPC (Transmit Power Control) in WLAN systems [2, 9, 12], which allows a WLAN device to use the minimum required power level in the transmit mode and is complementary to the power-management policies. In this paper, we propose a novel intelligent TPC mechanism, called *MiSer*, that minimizes the communication energy consumption in 802.11a/h systems.

1.1 Motivation and Key Contributions

The IEEE 802.11 [14] specifies two different MAC (Medium Access Control) schemes in WLANs: the contention-based DCF (Distributed Coordination Function) and the polling-based PCF (Point Coordination Function). At present, most 802.11-compliant products only implement the mandatory DCF. Thus, we only consider the DCF in this paper.

The IEEE 802.11 PHYs (physical layers) provide multiple transmission rates by employing different modulation and channel coding schemes. For example, the 802.11b PHY [16] provides 4 PHY rates from 1 to 11 Mbps at the 2.4 GHz band and most 802.11 devices available today in the market are based on this PHY. Another higher-speed PHY, the 802.11a PHY [15], has also been developed to extend the 802.11 operation in the 5 GHz U-NII (Unlicensed National Information Infrastructure) band and provides 8 PHY rates ranging from 6 to 54 Mbps. As the first-generation 802.11a products become available in the market, the 802.11a PHY receives increasing attention due mainly to its higher transmission rates as well as the cleaner 5 GHz operational band. Moreover, the emerging 802.11h standard [17], which is an extension to the cur-

rent 802.11 MAC and 802.11a PHY, provides a transmit-power reporting mechanism that makes intelligent TPC feasible at the MAC layer. Now, with the 802.11h getting close to its final standardization, it is important to have a well-designed TPC mechanism work with the 802.11a/h such that its TPC capability and multiple transmission rates can be fully exploited.

In this paper, based on the energy consumption analysis of an 802.11a/h DCF system, we propose a novel *per-frame-based* intelligent TPC mechanism, called *MiSer* (Minimum-energy transmission Strategy), assuming the knowledge of the network configuration and the wireless channel model. Obviously, the lower the transmit power or the higher the PHY rate (hence, the shorter the transmission time), the less energy consumed in one single transmission attempt, but more likely the transmission will fail, thus causing re-transmissions and eventually consuming more energy. So, there are inherent tradeoffs, and the key idea behind MiSer is to combine TPC with PHY rate adaptation and pre-establish a rate-power combination table indexed by the data transmission status quadruplet that consists of the data payload length, the path loss condition, and the frame retry counts. Each entry of the table is the optimal rate-power combination in the sense of maximizing the energy efficiency — which is defined as the ratio of the expected delivered data payload to the expected total energy consumption — under the corresponding data transmission status. At runtime, a wireless station determines the best transmit power as well as the proper PHY rate for each data transmission attempt by a simple table lookup, using the most up-to-date data transmission status as the index.

Note that, due to the contention nature of the DCF, the effectiveness of MiSer relies on the condition that applying TPC to data transmissions will not aggravate the "hidden nodes" problem or the interference in the network. Hence, like many other proposed TPC mechanisms [2, 12], MiSer exchanges RTS/CTS frames to reserve the medium before making each data transmission attempt. Moreover, we (i) investigate the relation among different radio ranges and TPC's effect on the interference in 802.11a/h systems, (ii) propose transmission of the CTS frames at a stronger power level to ameliorate the interference, and (iii) justify it by a theoretical analysis.

1.2 Related Work

In [21], the authors presented a scheme in which the most battery energy-efficient combination of FEC (Forward Error Correction) code and ARQ (Automatic Re-transmission reQuest) protocol is chosen and adapted over time for data transmissions without considering TPC.

A PARO (Power-Aware Routing Optimization) scheme was presented in [12] to achieve the energy-efficient routing in multi-hop wireless networks. Before the actual data transmission, PARO exchanges RTS/CTS frames at the maximum power level. Then, the subsequent Data/Ack frames may be transmitted at lower power levels to save energy. Another similar power control scheme was proposed in [2], where the transmit power level of the data frame is dynamically adjusted with help of an enhanced RTS/CTS mechanism that supports power control loop. In [9], the authors first showed the strong correlation among the packet size, the transmit power, and the energy consumption for 802.11 devices. Then, based on a theoretical analysis, they proposed a power control scheme to save energy by choosing the optimal transmit power levels for different packet sizes.

One common problem of the above power control schemes is that none of them considered PHY rate adaptation, a key component of MiSer. Since the 802.11 PHYs support multiple transmission rates, utilizing them adaptively by choosing the best PHY rate at a given time can enhance the system performance significantly, and in fact, our simulation results in Section 6 show that PHY rate adaptation is very effective in saving energy. Hence, PHY rate adaptation should be considered in conjunction with TPC.

The authors of [11, 23] proposed a lazy scheduling algorithm and an iterative MoveRight algorithm, respectively, to minimize the energy used to transmit packets from a wireless station to a single receiver or to multiple receivers. The key idea is to transmit packets over longer periods with lower transmit power as long as the deadline constraint is met. However, they assumed that the wireless channel is time-invariant and focused on devising optimal schedules for a wireless station to transmit multiple packets (sharing the same deadline constraint), which is quite different from the issues we address in this paper.

1.3 The Evolution of MiSer

We originated the research of energy-efficient WLAN operations on an 802.11a system under the (optional) PCF. Since the access to the wireless medium is centrally-controlled by the AP (Access Point), there is no "hidden nodes" problem or medium contention in a PCF system, which makes it easy to apply TPC to save energy. In [26], we derived the energy-consumption performance analytically for uplink data transmissions under the PCF and demonstrated the energy-efficient PCF operation via TPC and PHY rate adaptation.

It may seem reasonable to apply a similar idea under the (mandatory) DCF as well. However, as described in [13], if wireless stations are simply allowed to transmit at different power levels in a DCF system, the number of hidden terminals is likely to increase and the interference is aggravated, which, in turn, results in more transmission failures and re-transmissions, and hence, more energy will eventually be consumed. A natural way to deal with such problem is to exchange RTS/CTS frames before each data transmission attempt, which has been used in many proposed TPC mechanisms [2, 12].

Our preliminary study in [25] considered the simple infrastructure DCF system that includes an AP to provide both the connection to the wired network, if any, and the local relaying function within the system. Therefore, each wireless station must be able to hear the AP, and consequently, the hidden terminals are completely eliminated if RTS/CTS frames are exchanged before each data transmission attempt. Our simulation results showed the energy savings by TPC (with RTS/CTS support) in an infrastructure DCF system and confirmed the aggravated "hidden nodes" problem when TPC is applied directly to data transmissions without RTS/CTS support.

This problem becomes much more complicated in an ad hoc DCF system where the wireless stations, if within the communication range, communicate directly with each other. Since not every wireless station may be able to hear directly from all other stations, the RTS/CTS mechanism can not guarantee elimination of the hidden terminals. Moreover, applying TPC to data transmissions, even with RTS/CTS support, aggravates the interference in an ad hoc DCF system. MiSer reflects our latest research results on this topic and can be used in both infrastructure and ad hoc DCF systems.

1.4 Organization

The rest of this paper is organized as follows. For completeness, Section 2 briefly introduces the DCF of the IEEE 802.11 MAC as well as the IEEE 802.11a PHY. In Section 3, following a theoretical analysis of the relation among different radio ranges and TPC's effect on the interference in 802.11a/h systems, an enhanced RTS-

CTS-Data-Ack mechanism is proposed and justified to accommodate intelligent TPC. A generic energy consumption model of the WLAN device and the basic energy consumption computations in an 802.11a/h DCF system are presented in Section 4. Section 5 describes the details of MiSer and discusses the related implementation issues. Section 6 presents and evaluates the simulation results, and finally, the paper concludes with Section 7.

2. System Overview

2.1 DCF of the 802.11 MAC

The DCF [14], as the basic access scheme of the 802.11 MAC, achieves automatic medium sharing among compatible stations via the use of CSMA/CA (Carrier-Sense Multiple Access with Collision Avoidance). A wireless station is allowed to transmit only if its carrier-sense mechanism determines that the medium has been idle for at least DIFS (Distributed Inter-Frame Space) time. Moreover, in order to reduce the collision probability among multiple stations accessing the medium, a station is required to select a random backoff interval after deferral, or prior to attempting to transmit another frame after a successful transmission.

The SIFS (Short Inter-Frame Space), which is smaller than the DIFS, is the time interval used between transmissions within a frame exchange sequence, e.g., a two-way Data-Ack handshake or a four-way RTS-CTS-Data-Ack handshake. Using this small gap prevents other stations — which are required to wait for the medium to be idle for a longer gap (i.e., at least DIFS time) — from attempting to use the medium, thus giving priority to completion of the in-progress frame exchange. The timing of a successful four-way frame exchange is shown in Fig. 1. On the other hand, if a CTS (Ack) frame is not received due possibly to an erroneous reception of the preceding RTS (Data) frame, as shown in Figs. 2 and 3, the transmitter will contend again for the medium to re-transmit the frame after a CTS (Ack) timeout. Note that, in these figures, a crossed block represents an erroneous reception of the corresponding frame.

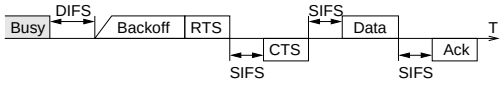

Figure 1: Timing of a successful four-way frame exchange under the DCF

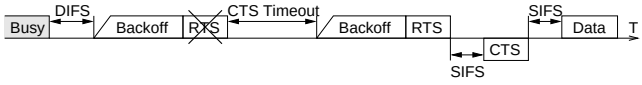

Figure 2: Re-transmission due to RTS transmission failure

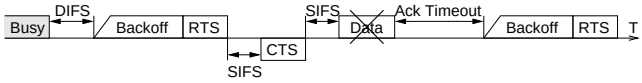

Figure 3: Re-transmission due to Data transmission failure

The DCF includes a virtual sensing mechanism, called the NAV (Network Allocation Vector), in addition to physical sensing. The NAV is a value that indicates to a station the remaining time before the wireless medium becomes available, and it is updated upon each RTS/CTS frame reception using the Duration/ID value carried in the frame header. By examining the NAV, a station avoids transmitting a frame that may interfere with the subsequent Data/Ack frame exchange even when the wireless medium appears to be idle according to physical sensing. Fig. 4 illustrates how the wireless stations adjust their NAVs during a four-way frame exchange.

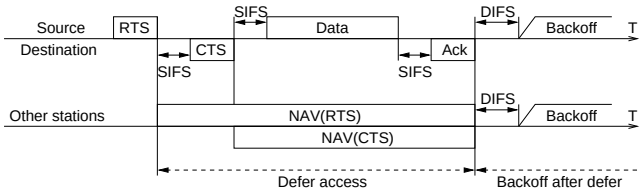

Figure 4: NAV setting during a four-way frame exchange

The 802.11 MAC requires that a wireless station maintain a short retry count (SRC) and a long retry count (LRC) for each data frame, and these counts are incremented and reset independently. When the RTS-CTS-Data-Ack handshake is used to transmit a data frame, SRC (LRC) is incremented every time an RTS (Data) transmission fails. The data frame is discarded when either SRC reaches *dot11ShortRetryLimit* or LRC reaches *dot11LongRetryLimit*. The default values of *dot11ShortRetryLimit* and *dot11LongRetryLimit* are 7 and 4, respectively. Note that both SRC and LRC are reset to 0 *only* after a successful data transmission or after a data frame is discarded.

2.2 The 802.11a PHY

The 802.11a PHY [15] is based on OFDM (Orthogonal Frequency Division Multiplexing) and provides 8 PHY rates with different modulation schemes and convolutional codes at the 5 GHz U-NII band. As listed in Table 1, the OFDM system provides a WLAN with capabilities of communicating at 6 to 54 Mbps. The frame exchange between MAC and PHY is under the control of the PLCP (Physical Layer Convergence Procedure) sublayer.

Table 1: Eight PHY Rates of the IEEE 802.11a OFDM PHY

PHY Rate	Modulation	Code Rate	BpS*
6 Mbps	BPSK	1/2	3
9 Mbps	BPSK	3/4	4.5
12 Mbps	QPSK	1/2	6
18 Mbps	QPSK	3/4	9
24 Mbps	16-QAM	1/2	12
36 Mbps	16-QAM	3/4	18
48 Mbps	64-QAM	2/3	24
54 Mbps	64-QAM	3/4	27

* Bytes per OFDM Symbol

3. Interference Analysis for 802.11(a/h) Systems

Applying TPC, which allows a WLAN device to use the minimum required power level in the transmit mode, is naturally an attractive idea to save battery energy and has been studied by many researchers [2, 9, 12].

MiSer is our intelligent TPC mechanism for 802.11a/h DCF systems, and due to the contention nature of the DCF, the effectiveness of MiSer relies on the condition that applying TPC to data transmissions will not aggravate the "hidden nodes" problem or the interference in the network. For this reason, like many other proposed TPC mechanisms [2, 12], MiSer exchanges RTS/CTS frames

before each data transmission attempt to deal with the "hidden nodes" problem. More importantly, it transmits the CTS frames at a stronger power level to ameliorate the potentially aggravated interference caused by TPC, which is justified by a theoretical analysis as follows. We first investigate the relation among different radio ranges and TPC's effect on the interference in 802.11(a/h) systems.

3.1 Radio Ranges in 802.11 Systems

In general, there are four different radio ranges in 802.11 systems: *transmission range*, *NAV set range*, *CCA busy range*, and *interference range*.

- *Transmission range* is central to the transmitter and represents the range within which the receiver station can receive a frame successfully, assuming no interference from neighboring stations. It varies with the data payload length, the PHY rate, the transmit power, the radio propagation property that determines the path loss, and the receiver-side noise level.
- *NAV set range* is the range within which the wireless stations can set the NAVs correctly based on the Duration/ID information carried in the RTS/CTS frames and will not interfere with the subsequent Data/Ack frame exchange. Since the RTS/CTS frames are always transmitted at a fixed rate (e.g., 6 Mbps in 802.11a/h systems), the NAV set range is independent of the data rate.
- *CCA busy range* is central to the transmitter and represents the range within which the wireless stations can physically sense the channel busy during the data transmission (by the transmitter) and then defer their own transmission attempts. There are two methods for a wireless station to report CCA (Clear Channel Assessment) busy. One is based on *carrier detection*, and the other is based on *energy detection* by which a wireless station will report a busy medium upon detection of any signal power above the ED (Energy Detection) threshold.
- *Interference range* is central to the receiver and represents the range within which the wireless stations are able to interfere with the reception of data frames at the receiver.

3.2 TPC's Effect on the Interference in 802.11 Systems

Fig. 5 sketches the different radio ranges when the transmitter (*T*) transmits a data frame to the receiver (*R*) using the RTS-CTS-Data-Ack handshake. NAV set range, CCA busy range, and interference range are shown as the light-, medium-, and dark-shaded areas, respectively. The NAV set range is actually the conjunction of the RTS transmission range and the CTS transmission range. Note that the radio ranges vary with 802.11 systems equipped with different PHYs.

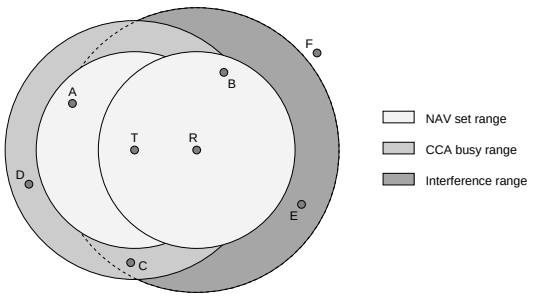

Figure 5: A sketch of the radio ranges during a four-way frame exchange

A, *B*, *C*, *D*, *E*, and *F* are the six neighboring stations. Clearly, *A*, *B*, *C*, *D*, and *F* will not interfere with the Data/Ack frame exchange, since *A* and *B* can set the NAVs correctly, *C* and *D* can physically sense the channel busy, and *F* is outside the interference range. On the other hand, *E* is not within either the NAV set range or the CCA busy range, but is close enough to the receiver (within the interference range) to cause the interference.

Now, let us see how the radio ranges are affected when TPC is applied on data transmissions. Since the kernel idea of TPC is to transmit a data frame at the minimum required power level, it may aggravate the interference in the following ways.

- *Scenario I:* The CCA busy range shrinks so that some neighboring stations that originally deferred their transmission attempts based on physical sensing may now interfere with the data frame reception (e.g., *C* in Fig. 5) or with the Ack frame reception (e.g., *C* and *D* in Fig. 5). This scenario may occur *only* when the original CCA busy range is larger than the NAV set range.
- *Scenario II:* The interference range is enlarged so that some neighboring stations (e.g., *F* in Fig. 5) that were originally outside the interference range, may now interfere with the data frame reception.

Having recognized the potential problem of aggravating the interference when applying TPC on data transmissions, we would like to design an intelligent TPC mechanism for 802.11a/h systems, which not only applies TPC on data transmissions to save energy, but, more importantly, ameliorates the interference as well.

3.3 NAV Set Range vs. CCA Busy Range in 802.11a/h Systems

According to the 802.11a standard [15], the *receiver minimum input level sensitivity* is defined as the received signal strength level at which the PER (Packet Error Rate) of a 1000-octet frame is less than 10%. It is rate-dependent and the different numbers for different PHY rates are listed in Table 91 of [15]. For example, the receiver minimum sensitivity level for 6 Mbps is -82 dBm. Since the length of an RTS/CTS frame is much shorter than 1000 octets and they are transmitted at the most robust 6 Mbps, the PER of an RTS/CTS frame at the minimum 6 Mbps sensitivity level (-82 dBm) is almost zero. Therefore, it is safe to say that the RTS/CTS transmission range in an 802.11a/h system corresponds to the minimum 6 Mbps sensitivity level (-82 dBm). Recall that the NAV set range is the conjunction of the RTS transmission range and the CTS transmission range.

On the other hand, the *CCA sensitivity* is defined (on Page 32 of [15]) as: "The start of a valid OFDM transmission at a receive level equal to or greater than the minimum 6 Mbps sensitivity (-82 dBm) shall cause CCA to indicate busy with a probability $> 90\%$ within 4 μs. If the preamble portion was missed, the receiver shall hold the CS (Carrier Sense) signal busy for any signal 20 dB above the minimum 6 Mbps sensitivity." Therefore, the CCA busy sensitivity levels based on carrier detection and energy detection are -82 dBm and -62 dBm, respectively, regardless of the data transmission rate.

We can make an important observation: *when the four-way handshake is used in an 802.11a/h system to transmit a data frame, the CCA busy range is completely covered by the NAV set range.* This unique feature of 802.11a/h systems is due to the fact that, unlike the 802.11b PHY, the 802.11a PHY's ED threshold is set 20 dB higher than the carrier detection threshold. Hence, the *Scenario I*

described in Section 3.2 will never occur in an 802.11a/h system, while it may cause serious interference problems in 802.11b systems.

3.4 NAV Set Range vs. Interference Range in 802.11a/h Systems

Since the signal power needed for interrupting a frame reception is much lower than that of delivering a frame successfully [34], under certain circumstances — especially, when TPC is used for data transmissions, as will be shown below — the interference range may be larger than the NAV set range. We now investigate the relation between the transmit power and the interference range when three different four-way frame exchange mechanisms are used.

3.4.1 RTS-CTS-Data-Ack

First, let us consider the conventional four-way handshake, where all the frames are transmitted at the same nominal power level ($\mathcal{P}_{nom}$).[1] As shown in Fig. 6, the distance between *T* and *R* is d. Let $d_{tx\_rc,6mbps}$ denote the radius of the RTS/CTS transmission range. So, we have

$$r_t = r_r = d_{tx\_rc,6mbps} \geqslant d. \tag{1}$$

Note that the CCA busy range is not shown in Fig. 6, as it is completely covered by the NAV set range in 802.11a/h systems.

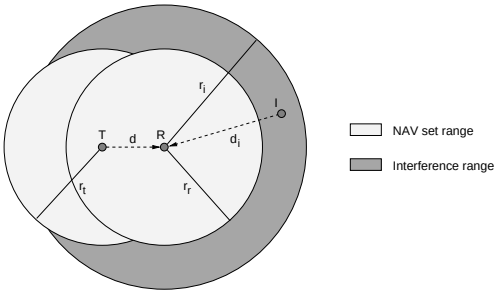

Figure 6: NAV set range vs. Interference range

The radius of the interference range can be determined as follows. Assume that, at the same time when *T* initiates a data frame (with payload ℓ) transmission (at rate x) to *R*, a neighboring station (*I*) with distance d_i away from *R* starts another transmission. Let $SIR_{th\_\ell,x}$ be the SIR (Signal-to-Interference Ratio) threshold above which the data frame can be successfully received. Therefore, an interference occurs if the following condition holds:

$$\begin{aligned} SIR_{th\_\ell,x} &\geqslant SIR \\ &= \mathcal{P}_{r,data} - \mathcal{P}_{r,int} \\ &= (\mathcal{P}_{t,data} - PL_d) - (\mathcal{P}_{t,int} - PL_{d_i}) \\ &= (\mathcal{P}_{nom} - PL_d) - (\mathcal{P}_{nom} - PL_{d_i}) \\ &= PL_{d_i} - PL_d \\ &= \left(\frac{d_i}{d}\right)^4 \qquad (2) \\ \iff d_i &\leqslant \sqrt[4]{SIR_{th\_\ell,x}} \cdot d. \qquad (3) \end{aligned}$$

$\mathcal{P}_{t,data}$, $\mathcal{P}_{r,data}$, $\mathcal{P}_{t,int}$, and $\mathcal{P}_{r,int}$ are the transmit power of the data frame, the received data signal strength, the transmit power of the interference signal, and the received interference signal strength (all in dBm), respectively. PL_d and PL_{d_i} are the path losses (in dB) over distances d and d_i, respectively. Eq. (2) is obtained by assuming the log-distance path loss model with path loss exponent of four [27], which is suitable for indoor office environments. Eq. (3) implies that, in order to interfere with the data frame reception, an interfering station must be within distance $\left(\sqrt[4]{SIR_{th\_\ell,x}} \cdot d\right)$ from the receiver, or equivalently, the radius of the interference range is

$$r_i = \sqrt[4]{SIR_{th\_\ell,x}} \cdot d. \tag{4}$$

We have two observations. First, when the conventional four-way handshake is used, the size of the interference range varies with the data payload length (ℓ), the transmission rate (x), and the distance (d) between the transmitter and the receiver. Only when d is larger than a certain value, the NAV set range will not be able to cover the interference range, i.e.,

$$d > \frac{d_{tx\_rc,6mbps}}{\sqrt[4]{SIR_{th\_\ell,x}}} \quad \Longrightarrow \quad r_i > r_r, \tag{5}$$

and then the neighboring stations that are inside the interference range but outside the NAV set range can interfere with the data frame reception. Second, the interference signal could be RTS, CTS, Data, or Ack frames.

3.4.2 RTS-CTS-Data(TPC)-Ack

Now, let us examine how the interference range is affected when we only apply TPC on data transmissions while keeping the transmit power of RTS, CTS, and Ack frames at the nominal level. So in this case,

$$\mathcal{P}'_{t,data} \leqslant \mathcal{P}_{nom}. \tag{6}$$

Consider the same configuration as shown in Fig. 6, and let $d_{tx\_\ell,x}$ denote the transmission range when a data frame with payload ℓ is transmitted at rate x using the nominal transmit power. Now, the condition for an interference to occur becomes

$$\begin{aligned} SIR_{th\_\ell,x} &\geqslant SIR \\ &= \mathcal{P}'_{r,data} - \mathcal{P}'_{r,int} \\ &= \left(\mathcal{P}'_{t,data} - PL_d\right) - \left(\mathcal{P}'_{t,int} - PL_{d_i}\right) \\ &= \left(\mathcal{P}_{nom} - PL_{d_{tx\_\ell,x}}\right) - \left(\mathcal{P}'_{t,int} - PL_{d_i}\right) \qquad (7) \\ &\geqslant \left(\mathcal{P}_{nom} - PL_{d_{tx\_\ell,x}}\right) - \left(\mathcal{P}_{nom} - PL_{d_i}\right) \\ &= PL_{d_i} - PL_{d_{tx\_\ell,x}}. \qquad (8) \end{aligned}$$

Eq. (7) is based on the fact that, when TPC is used for the data transmission, the transmitter adapts its transmit power in such a way that the received data signal strength is always kept at the minimum required level.

Note that, when the data frame carries a larger payload ($\ell\uparrow$) or is transmitted at a higher rate ($x\uparrow$), a higher receiver-side SIR is required to have a successful frame reception ($SIR_{th\_\ell,x}\uparrow$), and consequently, the frame transmission range shrinks ($d_{tx\_\ell,x}\downarrow$), yielding a smaller $PL_{d_{tx\_\ell,x}}$ value. The changes in $SIR_{th\_\ell,x}$ and $PL_{d_{tx\_\ell,x}}$ are similar. Therefore, Eq. (8) is equivalent to

$$\begin{aligned} SIR_{th\_rc,6mbps} &\geqslant PL_{d_i} - PL_{d_{tx\_rc,6mbps}} \\ \iff SIR_{th\_rc,6mbps} &\geqslant \left(\frac{d_i}{d_{tx\_rc,6mbps}}\right)^4 \\ \iff d_i &\leqslant \sqrt[4]{SIR_{th\_rc,6mbps}} \cdot d_{tx\_rc,6mbps}. \qquad (9) \end{aligned}$$

Hence, the radius of the interference range becomes

$$r'_i = \sqrt[4]{SIR_{th\_rc,6mbps}} \cdot d_{tx\_rc,6mbps}. \tag{10}$$

It is interesting to see that the size of the interference range is now independent of the data payload length (ℓ), the transmission rate

[1] In the following analysis, we let $\mathcal{P}_{nom}$ be 15 dBm, the nominal transmit power of the popular Agere ORiNOCO cards [3].

(x), and the distance (d) between the transmitter and the receiver, unlike when the conventional four-way handshake is used. Moreover, since $SIR_{th\_rc,6mbps}$ is larger than one, we have

$$r_i' > d_{tx\_rc,6mbps} = r_r, \tag{11}$$

which means that the interference range is always larger than the NAV set range. As a result, there are always some potential hidden terminals to interfere with the data frame reception, meaning that the interference is aggravated. This is actually the *Scenario II* described in Section 3.2. The interference signal could be RTS, CTS, Data, or Ack frames.

3.4.3 RTS-CTS(strong)-Data(TPC)-Ack

In order to deal with the aggravated interference problem caused by applying TPC on data transmissions, we propose to transmit the CTS frames at a stronger power level ($\mathcal{P}_{nom^+}$), which is 5 dB higher than, or equivalently, 3.16 times, the nominal transmit power. Since we let $\mathcal{P}_{nom}$ be 15 dBm, $\mathcal{P}_{nom^+}$ is 20 dBm and conforms to the 23 dBm transmit power limitation.[2] Now, with our enhanced four-way frame exchange mechanism, the NAV set range is enlarged to

$$r_r'' = \sqrt[4]{3.16} \cdot r_r = 1.33\, d_{tx\_rc,6mbps}. \tag{12}$$

Consider the same configuration as shown in Fig. 6. When the interference signal is RTS, Data, or Ack frames, since these frames are transmitted at or lower than the nominal power level, the analysis in Section *3.4.2* holds and we have

$$r_i'' = \sqrt[4]{SIR_{th\_rc,6mbps}} \cdot d_{tx\_rc,6mbps}. \tag{13}$$

Comparing Eq. (13) with Eq. (12), we can see that, as long as $SIR_{th\_rc,6mbps}$ is less than, or equal to, 5 dB — which is true according to [24][3] — the interference range is completely covered by the enlarged NAV set range, and hence, the data frame reception will never be interfered with by any RTS, Data, or Ack frames from neighboring stations.

On the other hand, when the interference signal is the stronger-power-transmitted CTS frames, the condition for an interference to occur becomes

$$\begin{aligned} SIR_{th\_\ell,x} &\geqslant SIR \\ &= \mathcal{P}''_{r,data} - \mathcal{P}''_{r,int(cts)} \\ &= \left(\mathcal{P}''_{t,data} - PL_d\right) - \left(\mathcal{P}''_{t,int(cts)} - PL_{d_i}\right) \\ &= \left(\mathcal{P}_{nom} - PL_{d_{tx\_\ell,x}}\right) - \left(\mathcal{P}_{nom^+} - PL_{d_i}\right) \\ &= PL_{d_i} - PL_{d_{tx\_\ell,x}} - 5 \text{ dB}. \end{aligned} \tag{14}$$

Following a similar argument as in Section *3.4.2*, Eq. (14) is equivalent to

$$\begin{aligned} & SIR_{th\_rc,6mbps} \geqslant PL_{d_i} - PL_{d_{tx\_rc,6mbps}} - 5 \text{ dB} \\ \iff\ & SIR_{th\_rc,6mbps} \geqslant \left(\frac{d_i}{d_{tx\_rc,6mbps}}\right)^4 \cdot \frac{1}{3.16} \\ \iff\ & d_i \leqslant \sqrt[4]{SIR_{th\_rc,6mbps}} \cdot 1.33\, d_{tx\_\ell,6mbps}, \end{aligned} \tag{15}$$

and the radius of the interference range, when the interference is caused by CTS frames, is

$$r_i'' = \sqrt[4]{SIR_{th\_rc,6mbps}} \cdot 1.33\, d_{tx\_rc,6mbps} > r_r''. \tag{16}$$

[2]According to the 802.11 standard [22], the maximum transmit power is limited to 200 mW (i.e., 23 dBm) for the middle band of the 5 GHz U-NII band, which is suitable for indoor environments.

[3]The error probability analysis in [24] showed that, when a data frame with 1152-octet payload is transmitted at 6 Mbps and the receiver-side SIR is larger than 5 dB, the PER of the frame is extremely small and, hence, negligible.

Therefore, the data frame reception may still be interfered with by the CTS signals. However, considering the fact that the CTS frames are normally much shorter than the data frames, such interference is not as severe as that caused by the data signals, which may occur when the conventional four-way handshake is used.

3.4.4 Summary

According to the above analysis, we can see that, our enhanced RTS-CTS(strong)-Data(TPC)-Ack mechanism is suitable to accommodate intelligent TPC in 802.11a/h systems, because it not only allows the data frames to be transmitted at lower power levels to save energy, but also ameliorates the potentially aggravated interference caused by TPC by transmitting the CTS frames at a stronger power level.

4. Energy Consumption Analysis of an 802.11a/h DCF System

Before delving into the details of MiSer, we will first analyze the average energy consumed by an 802.11a/h device when it is actively transmitting, receiving, or sensing the channel, i.e., when it is not in the doze mode. We also list the related notations.

4.1 Energy Consumption Model

Since we do not have access to the energy-consumption characteristics of any 802.11a-compliant product currently available in the market, we present a generic energy consumption model for WLAN devices for our analysis. It is based on the power characteristics of two popular 802.11b-compliant WLAN devices, the Agere ORiNOCO card [3] and the Intersil Prism II card [19].

Fig. 7 shows the simplified block diagram of a WLAN device. In general, the power consumption is different for the receive mode and the transmit mode, because different circuits are used in different modes. As shown in the figure, the RF power amplifier (PA) is active in the transmit mode only, while the receiving front end (e.g., the low noise amplifier in an Intersil Prism II card) is active only in the receive mode.

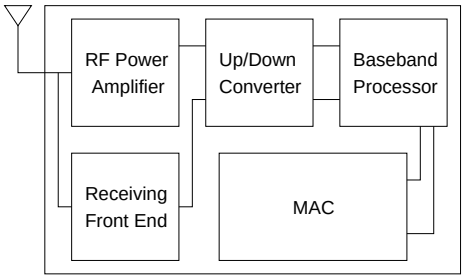

Figure 7: Simplified block diagram of a WLAN device

The power conversion efficiency (η) of a PA is defined as the ratio of the actual signal power emitted from the antenna, or the transmit power ($\mathcal{P}_t$), to the total power consumed by the PA ($\mathcal{P}_{pa}$). Basically, η is a function of $\mathcal{P}_t$, and a PA presents the following non-linearity feature: it achieves high efficiency at high transmit power levels, but the efficiency drops flat at low power levels. The E-P (Efficiency vs. transmit Power) curve varies with PA design. Based on the E-P curves given in [18, 28, 29], we assume an exponential E-P curve for the 5 GHz power amplifiers used in the 802.11a/h-compliant WLAN devices. Since we are only interested in how MiSer saves energy by combining TPC with PHY rate adaptation, not the exact amount of energy savings, this assumption has

little impact on the results and conclusions to be presented in Section 6.

Let $\mathcal{P}_{rec}$ denote the power consumption of the receiving front end. In general, $\mathcal{P}_{rec}$ is lower than $\mathcal{P}_{pa}$, and the difference becomes significant when the transmit power is high. Converter, baseband processor, and MAC are considered to be the common components of both receive and transmit circuits, and they are assumed to consume the same amount of power ($\mathcal{P}_{com}$) in both receive and transmit modes. Let $\mathcal{P}_{r\_mode}$ and $\mathcal{P}_{t\_mode}$ be the total power consumption in the receive and transmit modes, respectively. Then, we have

$$\begin{cases} \mathcal{P}_{r\_mode} = \mathcal{P}_{com} + \mathcal{P}_{rec}, \\ \mathcal{P}_{t\_mode}(\mathcal{P}_t) = \mathcal{P}_{com} + \mathcal{P}_{pa} = \mathcal{P}_{com} + \frac{\mathcal{P}_t}{\eta(\mathcal{P}_t)}. \end{cases} \tag{17}$$

Furthermore, we assume that, when a WLAN device is in the idle mode, it presents the same power consumption as when it is in the receive mode.

4.2 Energy Consumption Analysis

4.2.1 MAC/PHY Layer Overheads

As shown in Fig. 8, in the 802.11 MAC, each MAC data frame, or MPDU (MAC Protocol Data Unit), consists of the following components:[4] *MAC header*, *frame body* of variable length, and *FCS* (Frame Check Sequence). The MAC overheads due to the MAC header and the FCS are 28 octets in total. Besides, the frame sizes of an Ack frame, an RTS frame, and a CTS frame are 14, 20, and 14 octets, respectively.

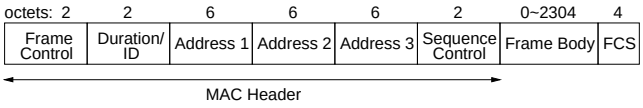

Figure 8: Frame format of a data frame MPDU

During the transmission, a PLCP preamble and a PLCP header are added to an MPDU to create a PPDU (PLCP Protocol Data Unit). The PPDU format of the 802.11a PHY is shown in Fig. 9, which includes PLCP preamble, PLCP header, MPDU (conveyed from MAC), tail bits, and pad bits, if necessary. The PLCP header except the SERVICE field, with the duration of *tPLCP_SIG*, constitutes a single OFDM symbol, which is transmitted with BPSK modulation and the rate-1/2 convolutional coding. Each OFDM symbol interval, denoted by *tSymbol*, is 4 μs. The 16-bit SERVICE field of the PLCP header and the MPDU (along with 6 tail bits and pad bits), represented by DATA, are transmitted at the data rate specified in the RATE field. Table 2 lists the related characteristics for the 802.11a PHY, where *tSlotTime*, *aCWmin*, and *aCWmax* will be discussed in next section.

Note that, while the data frames can be transmitted at any supported PHY rate, the RTS/CTS frames are always transmitted at 6 Mbps and the Ack frame is required to be transmitted at the highest rate in the BSS basic rate set[5] that is less than, or equal to, the rate of the data frame it is acknowledging. For example, if the BSS basic rate set is {6 Mbps, 12 Mbps, 24 Mbps} and a data frame is transmitted at 18 Mbps, the corresponding Ack frame will be transmitted at 12 Mbps.

[4]Actually, an additional field of "Address 4" appears in the WDS (Wireless Distribution System) data frames being distributed from one AP to another AP. However, since such WDS frames are rarely used, we do not consider the "Address 4" field in this paper. Besides, we do not consider the WEP (Wired Equivalent Privacy) option, which may introduce an extra 8-octet overhead.

[5]BSS (Basic Service Set) is the basic building block of an 802.11 system. It consists of a set of stations controlled by a single coordination function. BSS basic rate set is the set of rates that all the stations in a BSS are capable of using to receive/transmit frames from/to the wireless medium.

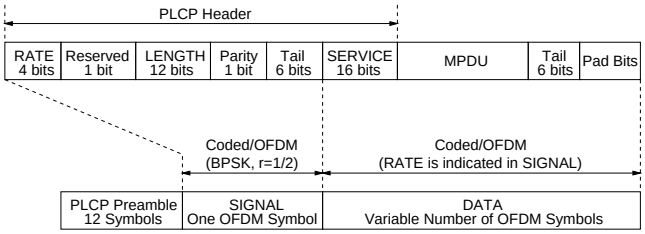

Figure 9: PPDU frame format of the 802.11a PHY

Table 2: The 802.11a PHY Characteristics

Characteristics	Value	Comments
tSlotTime	9 μs	Slot time
tSIFSTime	16 μs	SIFS time
tDIFSTime	34 μs	DIFS = SIFS + 2 $\times$ Slot
aCWmin	15	min contention window size
aCWmax	1023	max contention window size
tPLCPPreamble	16 μs	PLCP preamble duration
tPLCP_SIG	4 μs	PLCP SIGNAL field duration
tSymbol	4 μs	OFDM symbol interval

Based on the above analysis, to transmit a data frame with ℓ octets payload over the 802.11a PHY using PHY rate $\mathcal{R}$ and transmit power $\mathcal{P}_t$, the energy consumption is

$$\mathcal{E}_{data}(\ell, \mathcal{R}, \mathcal{P}_t) = \mathcal{T}_{data}(\ell, \mathcal{R}) \cdot \mathcal{P}_{t\_mode}(\mathcal{P}_t), \tag{18}$$

where the data transmission duration, $\mathcal{T}_{data}(\ell, \mathcal{R})$, is given by

$$\begin{aligned} \mathcal{T}_{data}(\ell, \mathcal{R}) &= \textit{tPLCPPreamble} + \textit{tPLCP\_SIG} \\ &\quad + \left\lceil \frac{28 + (16+6)/8 + \ell}{\textit{BpS}(\mathcal{R})} \right\rceil \cdot \textit{tSymbol} \\ &= 20\mu s + \left\lceil \frac{30.75 + \ell}{\textit{BpS}(\mathcal{R})} \right\rceil \cdot 4\mu s. \end{aligned} \tag{19}$$

Note that *BpS*($\mathcal{R}$), the Bytes-per-Symbol information for PHY rate $\mathcal{R}$, is given in Table 1. The energy consumed to receive the corresponding Ack frame is

$$\mathcal{E}_{ack} = \mathcal{T}_{ack}(\mathcal{R}') \cdot \mathcal{P}_{r\_mode}, \tag{20}$$

where the PHY rate used for the Ack transmission, $\mathcal{R}'$, is determined based on $\mathcal{R}$ according to the rule specified earlier, and the Ack transmission duration is

$$\mathcal{T}_{ack}(\mathcal{R}') = 20\mu s + \left\lceil \frac{16.75}{\textit{BpS}(\mathcal{R}')} \right\rceil \cdot 4\mu s. \tag{21}$$

Similarly, the energy consumption for an RTS frame transmission ($\mathcal{E}_{rts}$) using transmit power $\mathcal{P}_t$ and a CTS frame reception ($\mathcal{E}_{cts}$) can be calculated by

$$\mathcal{E}_{rts} = 52\mu s \cdot \mathcal{P}_{t\_mode}(\mathcal{P}_t), \tag{22}$$

and

$$\mathcal{E}_{cts} = 44\mu s \cdot \mathcal{P}_{r\_mode}, \tag{23}$$

respectively. Besides, We use $\mathcal{E}_{sifs}$ and $\mathcal{E}_{difs}$ to denote the energy consumptions of a WLAN device being idle for SIFS time

and DIFS time, respectively, and they can be calculated by

$$\mathcal{E}_{sifs} = \textit{tSIFSTime} \cdot \mathcal{P}_{r\_mode} = 16\mu s \cdot \mathcal{P}_{r\_mode}, \quad (24)$$

and

$$\mathcal{E}_{difs} = \textit{tDIFSTime} \cdot \mathcal{P}_{r\_mode} = 34\mu s \cdot \mathcal{P}_{r\_mode}. \quad (25)$$

4.2.2 Backoff Period

The random backoff interval is in the unit of *tSlotTime*, and this random integer is drawn from a uniform distribution over the interval [0, *CW*], where *CW* is the contention window size and its initial value is *aCWmin*. In the case of an unsuccessful RTS (Data) transmission, the backoff procedure will begin at the end of the CTS (Ack) timeout, and *CW* is updated to [2×(*CW*+1)−1]. Once *CW* reaches *aCWmax*, it will remain at this value until it is reset to *aCWmin*. In the case of a successful data transmission, the backoff procedure will begin at DIFS time after receiving the Ack frame, and the *CW* value is reset to *aCWmin* before the random backoff interval is selected. Note, however, that the *CW* value is *not* reset after a successful RTS transmission. Each station decrements its backoff counter every *tSlotTime* interval after the wireless medium is sensed to be idle for DIFS time. If the counter has not reached zero and one of the other stations starts transmitting, the station freezes its counter. When the counter finally reaches zero, the station starts its transmission.

Based on the above analysis, if the retry counts of a data frame are (SRC, LRC), which means that there have been SRC unsuccessful RTS transmission attempts and LRC unsuccessful data transmission attempts for this frame, then the average energy consumption of the WLAN device during the next backoff period consists of the following two parts: the energy consumption while the backoff counter is decrementing, which can be calculated by

$$\overline{\mathcal{E}}_{bkoff}(\text{SRC}, \text{LRC}) = \mathcal{P}_{r\_mode} \cdot \textit{tSlotTime} \cdot \frac{\min\left[2^{\text{SRC+LRC}} \cdot (\textit{aCWmin} + 1) - 1, \textit{aCWmax}\right]}{2}, \quad (26)$$

and the energy consumption while the backoff counter is frozen due to the busy medium, which is bounded by

$$\overline{\mathcal{E}}_{freeze} \leq \mathcal{P}_{r\_mode} \cdot (N_{sta} - 1) \cdot [P_{c,rts} \cdot 86\mu s + (1 - P_{c,rts}) \cdot (178\mu s + \mathcal{T}_{data}(1500, 6) + \mathcal{T}_{ack}(6))], \quad (27)$$

where N_{sta} is the number of contending stations in the network and $P_{c,rts}$ is the RTS collision probability. 86 μs and 178 μs represent an RTS transmission time plus a DIFS time, and an RTS transmission time plus a CTS transmission time plus three SIFS times plus a DIFS time, respectively.

Eq. (27) is derived based on the assumption that all the wireless stations are evenly distributed in the network and contending for the wireless medium fairly. So on average, during the backoff period, each of the contending stations attempts its RTS transmission once and succeeds with probability $(1-P_{c,rts})$. We also assume that the worst-case (longest) data transmission time corresponds to a data frame with 1500 octets payload — the Ethernet standard MTU (Maximum Transmission Unit) — transmitted at 6 Mbps.

5. MiSer

MiSer is motivated by [10] and is a simple table-driven approach. The basic idea is that the wireless station computes offline a rate-power combination table indexed by the data transmission status and each entry of the table is the optimal rate-power combination ($<\mathcal{R}^*, \mathcal{P}_t^*>$) in the sense of maximizing the energy efficiency ($\mathcal{J}$) under the corresponding data transmission status. The *data transmission status* is characterized by a quadruplet (ℓ, s, SRC, LRC), where ℓ is the data payload length, s is the path loss from the transmitter to the receiver, and (SRC, LRC) are the frame retry counts. The *energy efficiency* ($\mathcal{J}$) is defined as the ratio of the expected delivered data payload ($\mathcal{L}$) to the expected total energy consumption ($\mathcal{E}$). This table is then used at runtime to determine the proper PHY rate and transmit power for each data transmission attempt.

5.1 Step I: Offline Establishment of the Rate-Power Combination Table

We assume that the transmission error (due to background noise) probabilities of the RTS, CTS, and Ack frames are negligible because of their small frame sizes and robust transmission rates (refer to Section 3.3). Then, the table entries of the rate-power combination table are computed as follows.

First, consider the general case when

$$0 \leqslant \text{SRC} < \textit{dot11ShortRetryLimit} \quad (28)$$

and

$$0 \leqslant \text{LRC} < \textit{dot11LongRetryLimit}. \quad (29)$$

Assume that $<\mathcal{R}, \mathcal{P}_t>$ is selected for the data transmission attempt of status (ℓ, s, SRC, LRC). Also, assume that the future retransmission attempts, if any, will be made with the most energy-efficient transmission strategies as well. Clearly, the frame delivery is successful only if the RTS transmission succeeds without collision and the data transmission is error-free or results in correctable errors. Otherwise, the station has to re-contend for the medium to re-transmit the frame. In particular, if the delivery failure was due to the RTS collision, the frame retry counts become (SRC+1, LRC); if the delivery failure was due to the erroneous reception of the data frame, the frame retry counts become (SRC, LRC+1).

Based on the above observations, the expected delivered data payload ($\mathcal{L}$) and the expected total energy consumption ($\mathcal{E}$) can be calculated recursively as follows:

$$\begin{aligned}
&\mathcal{L}(\mathcal{R}, \mathcal{P}_t, \ell, s, \text{SRC}, \text{LRC}) = \\
&\quad (1 - P_{c,rts}) \cdot [1 - P_{e,data}(\mathcal{R}, \mathcal{P}_t, \ell, s)] \cdot \ell \\
&\quad + (1 - P_{c,rts}) \cdot P_{e,data}(\mathcal{R}, \mathcal{P}_t, \ell, s) \\
&\qquad \cdot \mathcal{L}(\mathcal{R}^*(\ell, s, \text{SRC}, \text{LRC+1}), \mathcal{P}_t^*(\ell, s, \text{SRC}, \text{LRC+1}), \\
&\qquad\quad \ell, s, \text{SRC}, \text{LRC+1}) \\
&\quad + P_{c,rts} \cdot \mathcal{L}(\mathcal{R}^*(\ell, s, \text{SRC+1}, \text{LRC}), \mathcal{P}_t^*(\ell, s, \text{SRC+1}, \text{LRC}), \\
&\qquad\quad \ell, s, \text{SRC+1}, \text{LRC}),
\end{aligned} \quad (30)$$

and

$$\begin{aligned}
&\mathcal{E}(\mathcal{R}, \mathcal{P}_t, \ell, s, \text{SRC}, \text{LRC}) = \\
&\quad \overline{\mathcal{E}}_{bkoff}(\text{SRC}, \text{LRC}) + \overline{\mathcal{E}}_{freeze} \\
&\quad + (1 - P_{c,rts}) \cdot [1 - P_{e,data}(\mathcal{R}, \mathcal{P}_t, \ell, s)] \\
&\qquad \cdot [\mathcal{E}_{rts-sifs-cts-sifs} + \mathcal{E}_{data}(\mathcal{R}, \mathcal{P}_t, \ell) + \mathcal{E}_{sifs} \\
&\qquad\quad + \mathcal{E}_{ack} + \mathcal{E}_{difs}] \\
&\quad + (1 - P_{c,rts}) \cdot P_{e,data}(\mathcal{R}, \mathcal{P}_t, \ell, s) \\
&\qquad \cdot [\mathcal{E}_{rts-sifs-cts-sifs} + \mathcal{E}_{data}(\mathcal{R}, \mathcal{P}_t, \ell) + \mathcal{E}_{ack_tout} \\
&\qquad\quad + \mathcal{E}(\mathcal{R}^*(\ell, s, \text{SRC}, \text{LRC+1}), \mathcal{P}_t^*(\ell, s, \text{SRC}, \text{LRC+1}), \\
&\qquad\quad\quad \ell, s, \text{SRC}, \text{LRC+1})] \\
&\quad + P_{c,rts} \cdot [\mathcal{E}_{rts} + \mathcal{E}_{cts_tout} \\
&\qquad + \mathcal{E}(\mathcal{R}^*(\ell, s, \text{SRC+1}, \text{LRC}), \mathcal{P}_t^*(\ell, s, \text{SRC+1}, \text{LRC}), \\
&\qquad\quad \ell, s, \text{SRC+1}, \text{LRC})].
\end{aligned} \quad (31)$$

$P_{c,rts}$ is the RTS collision probability and varies with the network configuration [5, 33]. $P_{e,data}$, the data transmission error probability, is a function of $\mathcal{R}$, $\mathcal{P}_t$, ℓ, and s, and varies with the wireless channel model [24]. Besides,

$$\mathcal{E}_{rts-sifs-cts-sifs} = \mathcal{E}_{rts} + 2 \cdot \mathcal{E}_{sifs} + \mathcal{E}_{cts}, \tag{32}$$

and $\overline{\mathcal{E}}_{bkoff}(\cdot)$, $\overline{\mathcal{E}}_{freeze}$, $\mathcal{E}_{data}(\cdot)$, $\mathcal{E}_{ack}$, $\mathcal{E}_{rts}$, $\mathcal{E}_{cts}$, $\mathcal{E}_{sifs}$, $\mathcal{E}_{difs}$ are given by Eqs. (26), (27), (18), (20), (22), (23), (24), and (25), respectively. Moreover, since an Ack (CTS) timeout is equal to a SIFS time, plus an Ack (CTS) transmission time, and plus a Slot time, we have

$$\mathcal{E}_{ack\_tout} = \mathcal{E}_{sifs} + \mathcal{E}_{ack} + \textit{tSlotTime} \cdot \mathcal{P}_{r\_mode}, \tag{33}$$

and

$$\mathcal{E}_{cts\_tout} = \mathcal{E}_{sifs} + \mathcal{E}_{cts} + \textit{tSlotTime} \cdot \mathcal{P}_{r\_mode}. \tag{34}$$

Hence, the energy efficiency ($\mathcal{J}$) is

$$\mathcal{J}(\mathcal{R}, \mathcal{P}_t, \ell, s, \text{SRC}, \text{LRC}) = \frac{\mathcal{L}(\mathcal{R}, \mathcal{P}_t, \ell, s, \text{SRC}, \text{LRC})}{\mathcal{E}(\mathcal{R}, \mathcal{P}_t, \ell, s, \text{SRC}, \text{LRC})}. \tag{35}$$

Since there are only finite choices for the PHY rate and the transmit power, we can calculate $\mathcal{J}$ for each rate-power combination, and the pair that maximizes $\mathcal{J}$ is then the most energy-efficient strategy for the data transmission attempt of status (ℓ, s, SRC, LRC):

$$\begin{aligned} &< \mathcal{R}^*(\ell, s, \text{SRC}, \text{LRC}),\ \mathcal{P}_t^*(\ell, s, \text{SRC}, \text{LRC}) > \\ &= \arg \max_{<\mathcal{R}, \mathcal{P}_t>} \mathcal{J}(\mathcal{R}, \mathcal{P}_t, \ell, s, \text{SRC}, \text{LRC}). \end{aligned} \tag{36}$$

Now, consider the special case when

$$\text{SRC} = \textit{dot11ShortRetryLimit} \tag{37}$$

and/or

$$\text{LRC} = \textit{dot11LongRetryLimit}. \tag{38}$$

Obviously, since at least one of the frame retry limits has been reached, the data frame will be discarded without any further transmission attempt. Hence, for any $<\mathcal{R}, \mathcal{P}_t>$, we always have

$$\begin{cases} \mathcal{E}(\mathcal{R}, \mathcal{P}_t, \ell, s, \textit{dot11ShortRetryLimit}, \text{LRC}) = 0, \\ \mathcal{L}(\mathcal{R}, \mathcal{P}_t, \ell, s, \textit{dot11ShortRetryLimit}, \text{LRC}) = 0, \end{cases} \tag{39}$$

and

$$\begin{cases} \mathcal{E}(\mathcal{R}, \mathcal{P}_t, \ell, s, \text{SRC}, \textit{dot11LongRetryLimit}) = 0, \\ \mathcal{L}(\mathcal{R}, \mathcal{P}_t, \ell, s, \text{SRC}, \textit{dot11LongRetryLimit}) = 0. \end{cases} \tag{40}$$

So, by using this special case as the boundary condition, we have fully specified the computation of the rate-power combination table by Eqs. (30), (31), (35), (36), (39), and (40).

5.2 Step II: Runtime Execution

Fig. 10 shows the pseudo-coded algorithm for MiSer. Before running the program, the wireless station computes the optimal rate-power combination for each set of data payload length (ℓ), path loss (s), and frame retry counts (SRC, LRC). Thus, a rate-power combination table is pre-established and ready for runtime use. The retry counts SRC_{curr} and LRC_{curr} for the frame at the header of the data queue are both set to 0. At runtime, the wireless station estimates the path loss between itself and the receiver, and then selects the rate-power combination $<\mathcal{R}_{curr}, \mathcal{P}_{t,curr}>$ for the current data transmission attempt by a simple table lookup. Note that the rate-power selection is made before the RTS frame is transmitted,

```
⟨ compute <R*, P_t*> for each set of ℓ, s, SRC, LRC ⟩;
SRC_max := dot11ShortRetryLimit;
LRC_max := dot11LongRetryLimit;
F := the frame at the header of the data queue;
ℓ_curr := DataPayloadLength(F);
SRC_curr := 0;   LRC_curr := 0;

while (the data queue is non-empty) {
  s_curr := the up-to-date path loss estimation;
  R_curr := R*(ℓ_curr, s_curr, SRC_curr, LRC_curr) ;
  P_{t,curr} := P_t*(ℓ_curr, s_curr, SRC_curr, LRC_curr) ;
  ⟨ an RTS frame is sent to reserve the medium ⟩;
  if (a CTS frame is received correctly)  then {
    ⟨ F is transmitted using <R_curr, P_{t,curr}> ⟩;
    if (an Ack frame is received correctly)  then {
      SRC_curr := 0;   LRC_curr := 0;
    }
    else  LRC_curr := LRC_curr + 1;
  }
  else  SRC_curr := SRC_curr + 1;
  if (SRC_curr ⩾ SRC_max || LRC_curr ⩾ LRC_max)  then {
    SRC_curr := 0;   LRC_curr := 0;
  }
  if (SRC_curr == 0 && LRC_curr == 0)  then {
    ⟨ remove the header frame from the data queue ⟩;
    ⟨ refresh F and ℓ_curr ⟩;
  }
}
```

Figure 10: Pseudo-code of MiSer

so that the Duration/ID information carried in the RTS frame can be properly set according to the PHY rate selection.

As shown in the pseudo-code, if an RTS/CTS frame exchange successfully reserves the wireless medium and an Ack frame is received correctly within the Ack timeout, the wireless station knows that the previous data transmission attempt was successful, and resets both retry counts to 0; else, either SRC_{curr} or LRC_{curr} is increased and the wireless station will re-select the rate-power combination for the next transmission attempt of the data frame. If the data frame cannot be successfully delivered after SRC_{max} medium reservation attempts or LRC_{max} data transmission attempts, the frame will be dropped and both SRC_{curr} and LRC_{curr} are reset to 0 for the next frame waiting in the data queue.

One important aspect of MiSer is that it shifts the computation burden offline, and hence, simplifies the runtime execution significantly. Therefore, embedding MiSer at the MAC layer has little effect on the performance of higher-layer applications, which is a desirable feature for any MAC-layer enhancement.

5.3 Implementation Issues

5.3.1 Table Establishment

As described in Section 5.1, in order to establish the rate-power combination table, a wireless station needs the following information:

- *Network configuration* that indicates the number of contending stations (N_{sta}) and determines the RTS collision probability ($P_{c,rts}$);
- *Wireless channel model* that determines the error performances of the PHY rates ($P_{e,data}$).

There have been a number of papers dealing with the problems of estimating the network configuration [6, 7] or building accurate

wireless channel models [4, 8, 32, 35], which, however, are not the focus of this paper. Instead, we propose a simple and effective TPC mechanism by assuming that the wireless station either has the required knowledge *a priori* or can estimate them.

5.3.2 Path Loss Estimation

At runtime, in order to look up the pre-established rate-power combination table to determine the best transmission strategy for each data frame, a wireless station has to estimate the path loss between itself and the receiver. We have developed a simple path loss estimation scheme, based on the upcoming 802.11h standard [17], as a possible solution.

The 802.11h standard is an extension to the current 802.11 MAC and 802.11a PHY, and one of the key improvements in 802.11h is to enable a wireless station to report its transmit power information in the newly-defined TPC Report element, which includes a Transmit Power field and a Link Margin field. The Transmit Power field simply contains the transmit power (in dBm) used to transmit the frame containing the TPC Report element, while the Link Margin field contains the link margin (in dB) calculated as the ratio of the received signal strength to the minimum desired by the station.

As specified in the 802.11h standard, the AP in an infrastructure network or a wireless station in an ad hoc network will autonomously include a TPC Report element with the Link Margin field set to zero and containing its transmit power information in the Transmit Power field in any Beacon or Probe Response frame it transmits. A wireless station keeps track of the path loss to the AP, if within an infrastructure network,[6] or the path loss to each neighboring station, if within an ad hoc network, and whenever it receives a Beacon or Probe Response frame, it updates the corresponding path loss value. That is, with the knowledge of the received signal strength (in dBm) via RSSI (Receive Signal Strength Indicator) as well as the transmit power (in dBm) via the TPC Report element found in the frame, the wireless station can calculate the path loss (in dB) from the sending station to itself by performing the simple subtraction. Note that RSSI is one of the RXVECTOR parameters, which is measured and passed to the MAC by the PHY and indicates the energy observed at the antenna used to receive the current frame. Basically, the path loss value(s) maintained in this manner can be used by the wireless station to determine its best transmission strategy.

This path loss estimation scheme is reasonable since with 802.11 systems, the same frequency channel is used for all transmissions in a time-division duplex manner, and hence, the channel characteristics in terms of path loss for both directions are likely to be similar. Moreover, since the Beacon frames are transmitted periodically and frequently, a wireless station is able to update the path loss value(s) in a timely manner.

6. Performance Evaluation

We evaluate the effectiveness of MiSer by using the ns-2 simulator [1] after enhancing the original 802.11 DCF module of ns-2 to support the 802.11a/h PHY, PHY rate adaptation, and TPC.

6.1 Simulation Setup

In the simulation, we use 15 dBm as the nominal transmit power, and a TPC-enabled 802.11a/h device is allowed to choose any one of the 31 power levels (from -15 dBm to 15 dBm with 1 dBm gaps) to transmit a data frame. We assume an AWGN (Additive White Gaussian Noise) wireless channel model and the background noise level is set to -93 dBm. The exponential E-P curve for the 5 GHz PA of the simulated 802.11a/h devices is

$$\eta(\mathcal{P}_t) = 0.02 \cdot 5^{\frac{\mathcal{P}_t}{15}}, \tag{41}$$

where $\mathcal{P}_t$ is in dBm. Besides, we use a log-distance path loss model with path loss exponent of four to simulate the indoor office environment, and set the carrier sensing threshold to -91 dBm, meaning that, when the distance between two stations is larger than 28.6 meters, the resulting path loss is larger than 106 (= 15 + 91) dB and these two stations are hidden to each other.

We evaluate five testing schemes: the proposed intelligent TPC mechanism (MiSer), the PHY rate adaptation scheme without TPC (RA), and three single-rate TPC schemes using PHY rate 6 Mbps (Tpc/R6), 24 Mbps (Tpc/R24), and 54 Mbps (Tpc/R54), respectively. These schemes are compared with each other in terms of the delivered data per unit of energy consumption (in MBits/Joule), which is calculated as the ratio of the total amount of data delivered by the transmitter stations over their total energy consumption. Note that the larger this value, the more energy-efficient a scheme gets. We also compare the aggregate goodput (in Mbps) of these schemes.

We conduct the simulation with various network topologies, station mobility patterns, and data payload lengths. Each simulation run lasts 10 seconds in an 802.11a/h system with 8 transmitter stations contending for the shared medium. Each station transmits in a greedy mode, i.e., its data queue is never empty, and all the data frames are transmitted without fragmentation. The frame size is 1500 octets unless specified otherwise.

6.2 MiSer's Rate-Power Combination Table

Recall that MiSer's rate-power combination table is indexed by (ℓ, s, SRC, LRC), and hence, is four-dimensional. Fig. 11 shows a snapshot of this table when ℓ = 1500 and (SRC, LRC) = (0, 0).

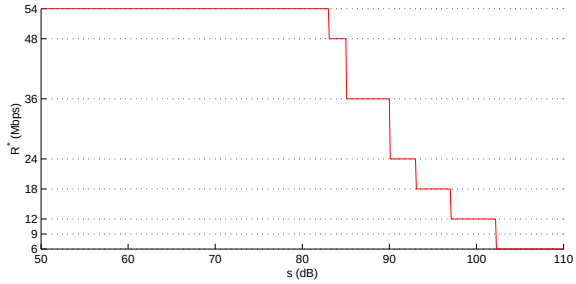

(a) PHY rate selection

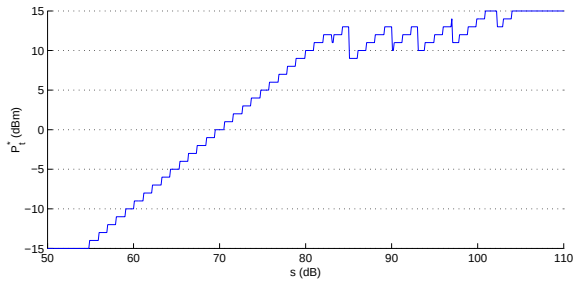

(b) transmit power selection

Figure 11: A snap shot of MiSer's rate-power combination table when ℓ = 1500 and (SRC, LRC) = (0, 0)

[6] In an infrastructure network, if a wireless station wants to communicate with another station, the frames must be first sent to the AP, and then from the AP to the destination [22]. Therefore, a wireless station only needs to keep track of the path loss between itself and the AP.

The optimal combinations of PHY rate and transmit power, which achieve the most energy-efficient data communications, under different path loss (s) conditions are shown in Fig. 11(a) and (b), respectively. For example, when s = 80 dB, this figure reads that <54 Mbps, 9 dBm> is the most energy-efficient transmission strategy.

We make two observations from Fig. 11. First, when the path loss is large, the lower PHY rates are preferred as they are more robust and have better error performances. On the other hand, when the path loss is small, higher PHY rates are used to save energy since the duration of a single transmission attempt is shorter. Second, a low transmit power does not necessarily save energy. This is because, with the same PHY rate, using a lower transmit power may lead to less energy consumption in a single transmission attempt, but the resultant low SNR (Signal-to-Noise Ratio) at the receiver side may cause more re-transmissions and, hence, more total energy consumption.

The snapshots for other ℓ and (SRC, LRC) values can be viewed approximately as shifted versions of Fig. 11. In general, when a data frame carried a larger payload ($\ell\uparrow$) or less transmission attempts remain for a data frame (SRC$\uparrow$ and/or LRC$\uparrow$), the figure shifts left and a more conservative combination (i.e., lower rate and/or higher power) is selected under the same path loss condition; otherwise, it shifts right.

Note that RA's rate adaptation table or Tpc/Rx's (x = 6, 24, or 54) power adaptation table are computed in the same way as that of MiSer's rate-power combination table, except fixing the transmit power to 15 dBm or the transmission rate to x Mbps, respectively.

6.3 Simulation Results

6.3.1 Star topologies with varying radius

We first compare the testing schemes in the star-topology networks, where 8 transmitter stations are evenly spaced on a circle around one common receiver with the radius of r ($1 \leq r \leq 28$) meters, and all the stations are static. Although ideal star-topology networks are rarely found in a real world, the simulation results plotted in Fig. 12 help us understand better how TPC adapts to the path loss variation and why MiSer is superior to all other simulated transmission strategies, thanks to the symmetric station deployment of star-topology networks, and hence, are valuable.

In general, as r increases, both the aggregate goodput and the delivered data per Joule decrease for all testing schemes. This is because more robust transmission strategies (i.e., lower rate and/or higher power) are used to deal with the increasing number of hidden terminals and a larger path loss between the transmitter and the receiver. However, different schemes show different decreasing curves determined by their respective design philosophies, which are discussed next. In order to have a better understanding of the figure, we list, in Table 3, the rate-power selections by each testing scheme, when r = 5, 9, 12, and 28, respectively.

Table 3: Example Rate-Power Selections (ℓ = 1500 and (SRC, LRC) = (0, 0))

r (m)	rate-power selection (<Mbps, dBm>)			
	5	9	12	28
MiSer	<54, 5>	<36, 9>	<24, 11>	<6, 15>
RA	<54, 15>	<54, 15>	<36, 15>	<6, 15>
Tpc/R6	<6, -13>	<6, -3>	<6, 2>	<6, 15>
Tpc/R24	<24, -3>	<24, 6>	<24, 11>	<24, 15>
Tpc/R54	<54, 5>	<54, 15>	<54, 15>	<54, 15>

RA achieves the highest aggregate goodput because its constant use of the strong 15 dBm transmit power allows it to choose the highest possible rate to transmit a data frame. On the other hand, since RA does not support TPC, so even within a small network, it still has to transmit a frame using a higher power than necessary over a short distance, hence consuming more energy. For example, as shown in Table 3, when r = 5, MiSer selects the same 54 Mbps rate as RA, but a much lower tranmit power level at 5 dBm. As a result, RA yields much lower delivered data per Joule than MiSer when r is small.

Tpc/R6 transmits all the data frames at the lowest 6 Mbps, and hence, results in the lowest aggregate goodput when r is small. As r increases, Tpc/R6 adjusts its transmit power adaptively such that the receiver-side SNR is maintained at a relatively stable level. For example, as shown in Table 3, when r increases from 5 to 9, 12, and 28, Tpc/R6 increases its transmit power from -13 dBm to -3 dBm, 2 dBm, and 15 dBm, respectively. Therefore, combined with rate 6 Mbps' strong error-correcting capability, Tpc/R6 shows an almost flat aggregate-goodput curve but a decreasing curve for the delivered data per Joule until r = 28, when even the most conservative combination of 6 Mbps and 15 dBm is still not robust enough to combat the resulting high path loss.

Tpc/R54 transmits all the data frames at the highest 54 Mbps. Similar to Tpc/R6, it also has a flat aggregate-goodput curve when r is small. However, due to rate 54 Mbps' poorest error-correcting capability, the aggregate-goodput curve starts dipping at a much smaller r value of 10. Actually, when $r > 10$, all the transmission attempts fail and the aggregate goodput drops to zero. Similar observations can be made for Tpc/R24 as well, which is a compromise between Tpc/R6 and Tpc/R54.

So we can see that, because of fixing the transmission rate, a single-rate TPC scheme either suffers a reduced transmission range (e.g., Tpc/R24 and Tpc/R54) or has to stick with a low transmission rate (e.g., Tpc/R6).

MiSer achieves the highest delivered data per Joule because of its adaptive use of (i) the energy-efficient combination of high rate and low power when r is small, and (ii) the robust combination of low rate and high power when r is large. The key idea is to select the optimal rate-power combination, rather than the PHY rate or the transmit power alone, to minimize the energy consumption. Therefore, under certain path loss conditions (e.g., r = 9 in Table 3), MiSer may choose a lower rate than RA but with weaker transmit power. As a result, MiSer shows an aggregate goodput curve slightly lower than that of RA. Note that MiSer has the same transmission range as RA and Tpc/R6, since a transmitter station that supports MiSer can always lower the PHY rate and/or increase the transmit power, whenever necessary, to communicate with a far-away receiver station. Another observation in Fig. 12 is that, when 6 Mbps (or 24 Mbps, 54 Mbps) or 15 dBm is part of the optimal rate-power selections, MiSer is indeed equivalent to Tpc/R6 (or Tpc/R24, Tpc/R54) or RA, which is evidenced by the partial overlapping in both their aggregate-goodput curves and their curves for the delivered data per Joule.

6.3.2 Random topologies with 50 different scenarios

We also evaluate and compare the performances of the testing schemes in randomly-generated network topologies: the 8 transmitter stations and their (different) respective receivers are randomly placed within a (40 m $\times$ 40 m) flat area, and all the stations are static. We simulate 50 different scenarios and the results are plotted in Fig. 13.

We have three observations. First, MiSer and RA are significantly better than the single-rate TPC schemes, in terms of both the

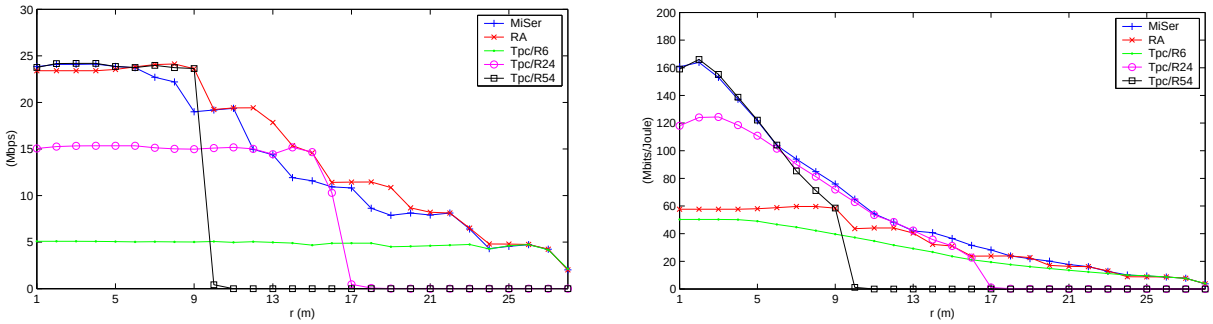

(a) aggregate goodput (b) delivered data per unit of energy consumption

Figure 12: Comparison for static star-topology networks (various radius)

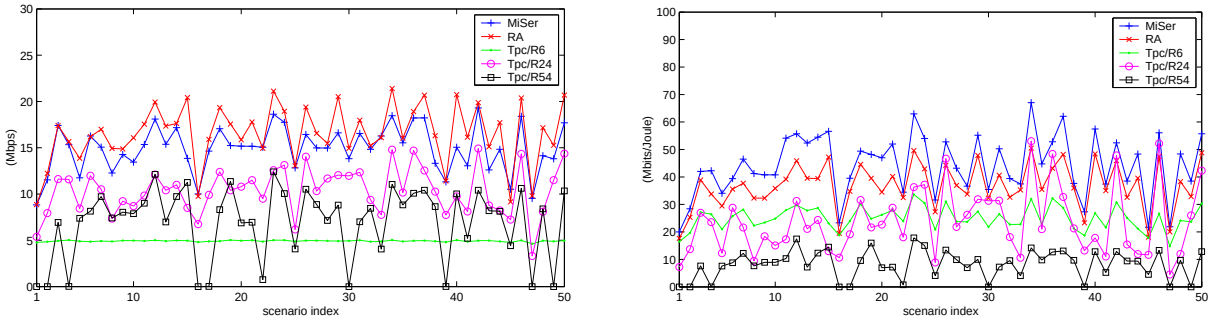

(a) aggregate goodput (b) delivered data per unit of energy consumption

Figure 13: Comparison for static random-topology networks (50 different scenarios)

aggregate goodput and the delivered data per Joule, in each simulated random topology. This is because the inevitable low transmission rate or reduced transmission range of a single-rate TPC scheme, where the latter may cause more potential transmission failures, results in poor aggregate-goodput and energy-efficiency performances. On the other hand, both MiSer and RA are able to perform PHY rate adaptation, which adjusts the transmission rate dynamically to the path loss variation.

Second, MiSer achieves comparable aggregate goodput with RA while delivering about 20% (on average) more data per unit of energy consumption than RA. Actually, the energy saving by MiSer over RA could be more significant if the network size is smaller. This is because, in a smaller network, the transmitter and the receiver are, on average, closer to each other, which corresponds to a smaller path loss value. As a result, MiSer may choose a much lower transmit power (than 15 dBm) to transmit a frame, thus saving more energy. On the other hand, when the network size gets larger, the energy-efficiency performances of MiSer and RA become comparable.

Third, Tpc/R6 produces near-constant aggregate goodput regardless of the network topology, which is consistent with a similar observation in Fig. 12. Besides, unlike in the small star-topology networks, where Tpc/R54 has the best energy performance, Tpc/R54 has the lowest delivered data per Joule in every scenario due to the arbitrary station locations in random-topology networks. Particularly, in 10 of the 50 simulated scenarios, Tpc/R54 results in almost zero aggregate goodput.

6.3.3 Random topologies with varying mobility

Fig. 14 shows the simulation results for random-topology networks with various station mobility. The simulated mobility patterns are specified by the maximum moving speeds of a wireless station, which are 0.5, 1, 2, and 4 m/s. Each point in the figure is averaged over 50 simulation runs with the same mobility pattern.

One important observation from the figure is that all the testing schemes are relatively insensitive to station mobility. This observation is surprising at the first sight, but reasonable for the following reason. Recall that an 802.11a/h device updates its path loss conditions to the neighboring stations upon each Beacon reception and the typical value of the Beacon interval is 100 ms. Therefore, even with the maximum speed of 4 m/s, which is considered very fast for indoor movements, the location difference of a wireless station between two path loss updates is 0.2 meters on average, which has little effect on the path loss conditions and the subsequent rate-power selections.

6.3.4 Random topologies with varying data payloads

Fig. 15 shows the simulation results for random-topology networks with various data payloads. The simulated data payload lengths are 32, 64, 128, 256, 512, 1024, and 1500 octets. Again, each point in the figure is averaged over 50 simulation runs.

Since the RTS/CTS frames are always transmitted at 6 Mbps, the RTS/CTS overhead per data transmission attempt is independent of the payload length. Moreover, as discussed in Section *4.2.1*, there are a number of fixed per-frame overheads such as the MAC header, the FCS, the PLCP preamble/header, and etc. Hence, both the aggregate goodput and the delivered data per Joule increase with the data payload length for all testing schemes. As expected, MiSer has the best energy-efficiency performance, and the gap between MiSer and RA becomes bigger as the data payload length increases. This is because, with the same PHY rate, a larger data payload results in a longer transmission time, during which MiSer may use low

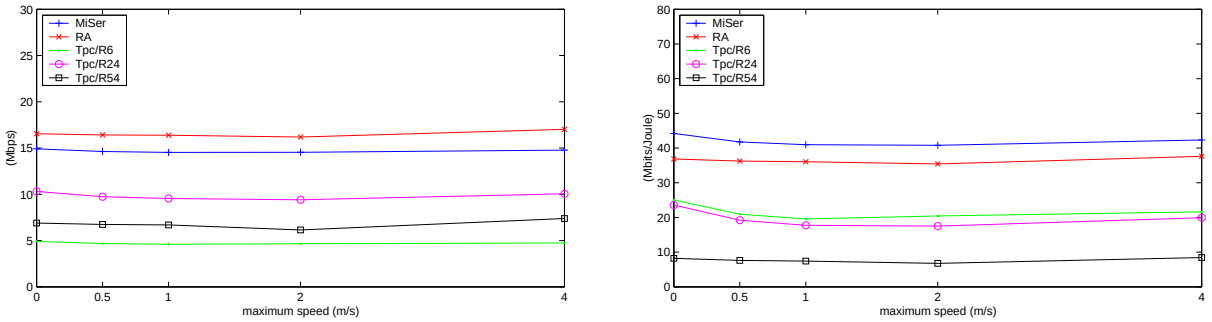

(a) aggregate goodput (b) delivered data per unit of energy consumption

Figure 14: Comparison for various station mobility patterns (average over 50 random topologies)

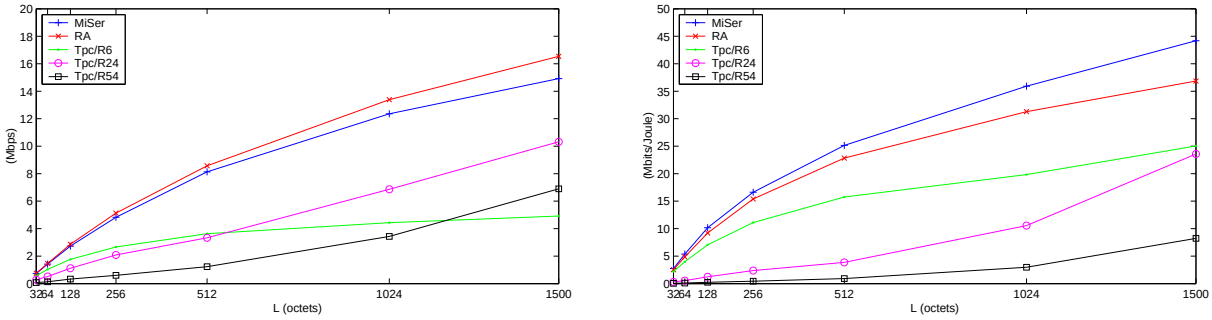

(a) aggregate goodput (b) delivered data per unit of energy consumption

Figure 15: Comparison for various data payloads (average over 50 random topologies)

transmit power to save more energy. Moreover, RA outperforms single-rate TPC schemes in terms of both goodput and energy consumption due to PHY rate adaptation.

It is interesting to see that the aggregate goodput curves of three single-rate TPC schemes intersect with each other in Fig. 15(a). When the data payload is less than 600 octets, Tpc/R6 yields the best goodput performance, while, when the data payload increases to 1500 octets, both Tpc/R24 and Tpc/R54 achieve better aggregate goodput than Tpc/R6, however, with much higher transmit power. This is because the strong error-correcting capability of rate 6 Mbps allows Tpc/R6 to transmit a large-payload data frame at a very low power level. In Fig. 15(b), when $\ell = 1500$, both Tpc/R24 and Tpc/R54 have smaller values of the delivered data per Joule than Tpc/R6, which, in turn, supports the above explanation. Note that, under different network configurations, the relative positions of these three aggregate goodput curves may vary.

6.4 Summary

Based on the observations from the simulation results, we summarize the effectiveness of MiSer as follows:

- MiSer is significantly better than any other scheme that simply adapts the PHY rate or adjusts the transmit power;
- PHY rate adaptation is very effective in saving energy and plays an important role in MiSer;
- Applying MiSer does not affect the transmission range;
- MiSer is insensitive to station mobility;
- MiSer is most suitable for data communications with large data payloads.

7. Conclusion and Future Work

In this paper, we propose a novel intelligent TPC mechanism, called *MiSer* (Minimum-energy transmission Strategy), as an optimal solution to the problem of minimizing the communication energy consumption in 802.11a/h systems. The key idea of MiSer is to combine TPC with PHY rate adaptation, so that the most energy-efficient rate-power combination can be adaptively selected for each data transmission attempt. It establishes an optimal rate-power combination table before the communication starts, which shifts the computation burden offline, and hence, simplifies the runtime execution (to simple table lookups) significantly.

The effectiveness of MiSer relies on the condition that applying TPC on data transmissions will not aggravate the "hidden nodes" problem and the interference in the network. So, MiSer (i) exchanges RTS/CTS frames before each data transmission attempt to deal with the "hidden nodes" problem, and (ii) transmits the CTS frames at a stronger power level to ameliorate the interference. The latter is justified by a rigorous analysis of the relation among different radio ranges and TPC's effect on the interference in 802.11a/h systems. Our in-depth simulation shows that MiSer is significantly better than single-rate TPC schemes and delivers about 20% more data per unit of energy consumption than the PHY rate adaptation scheme without TPC.

Since MiSer is designed as an intelligent TPC mechanism used in the transmit mode, it is complementary to the power-management policies that force a wireless device to enter the power-saving doze mode at appropriate moments to save battery energy. However, a simple combination of two may not necessarily result in the best energy-efficiency performance. For example, when the network load is light and the traffic is bursty, a wireless station may want to use RA instead of MiSer to finish the frame transmissions as

soon as possible, and then have the opportunity to enter the doze mode earlier to save more energy. Our future work includes the design of an ultimate optimal transmission strategy, which takes into consideration the impact of the power-saving doze mode on the rate-power selections in the transmit mode.

Acknowledgments

The authors would like to thank Danlu Zhang at Qualcomm and the anonymous reviewers for their helpful comments on an earlier version of this paper.

Appendix

A list of abbreviations and acronyms used in the paper (in the alphabetic order):

Ack	*Acknowledgment*
AP	*Access Point*
ARQ	*Automatic Re-transmission reQuest*
BpS	*Bytes per Symbol*
BPSK	*Binary Phase Shift Keying*
BSS	*Basic Service Set*
CCA	*Clear Channel Assessment*
CSMA/CA	*Carrier-Sense Multiple Access with Collision Avoidance*
DCF	*Distributed Coordination Function*
DIFS	*Distributed Inter-Frame Space*
ED	*Energy Detection*
E-P	*Efficiency vs. transmit Power*
FCS	*Frame Check Sequence*
FEC	*Forward Error Correction*
LRC	*Long Retry Count*
MAC	*Medium Access Control*
MiSer	*Minimum-energy transmission Strategy*
MPDU	*MAC Protocol Data Unit*
MTU	*Maximum Transmission Unit*
NAV	*Network Allocation Vector*
OFDM	*Orthogonal Frequency Division Multiplexing*
PA	*Power Amplifier*
PCF	*Point Coordination Function*
PER	*Packet Error Rate*
PHY	*Physical Layer*
PLCP	*Physical Layer Convergence Procedure*
PPDU	*PLCP Protocol Data Unit*
QAM	*Quadrature Amplitude Modulation*
QPSK	*Quadrature Phase Shift Keying*
RSSI	*Receive Signal Strength Indicator*
RTS/CTS	*Request-To-Send/Clear-To-Send*
SIFS	*Short Inter-Frame Space*
SIR	*Signal-to-Interference Ratio*
SNR	*Signal-to-Noise Ratio*
SRC	*Short Retry Count*
TPC	*Transmit Power Control*
U-NII	*Unlicensed National Information Infrastructure*
WDS	*Wireless Distributed System*
WEP	*Wired Equivalent Privacy*
WLAN	*Wireless Local-Area Network*

References

[1] The Network Simulator – ns-2. http://www.isi.edu/nsnam/ns/. Online Link.

[2] S. Agarwal, S. V. Krishnamurthy, R. K. Katz, and S. K. Dao. Distributed Power Control in Ad-Hoc Wireless Networks. In *Proc. IEEE PIMRC'01*, pages 59–66, 2001.

[3] Agere Systems. *User's Guide for ORiNOCO PC Card*, Sep. 2000.

[4] P. Bergamo, D. Maniezzo, A. Giovanardi, G. Mazzini, and M. Zorzi. An Improved Markov Chain Description for Fading Processes. In *Proc. IEEE ICC'02*, volume 3, pages 1347–1351, New York City, NY, Apr. 2002.

[5] G. Bianchi. Performance Analysis of the IEEE 802.11 Distributed Coordination Function. *IEEE Journal on Selected Areas in Communications*, 18(3):535–547, Mar. 2000.

[6] G. Bianchi, L. Fratta, and M. Oliveri. Performance Evaluation and Enhancement of the CSMA/CA MAC Protocol for 802.11 Wireless LANs. In *Proc. IEEE PIMRC*, pages 392–396, Taipei, Taiwan, Oct. 1996.

[7] F. Cali, M. Conti, and E. Gregori. Dynamic Tuning of the IEEE 802.11 Protocol to Achieve a Theoretical Throughput Limit. *IEEE/ACM Transactions on Networking*, 8(6):785–799, Dec. 2000.

[8] J.-P. Ebert and A. Willig. A Gilbert-Elliot Bit Error Model and the Efficient Use in Packet Level Simulation. TKN Technical Report TKN-99-002, Technical University Berlin, Telecommunication Networks Group, Berlin, Germany, Mar. 1999.

[9] J.-P. Ebert and A. Wolisz. Combined Tuning of RF Power and Medium Access Control for WLANs. *Mobile Networks & Applications*, 5(6):417–426, Sep. 2001.

[10] M. Elaoud and P. Ramanathan. Adaptive Use of Error-Correcting Codes for Real-time Communication in Wireless Networks. In *Proc. IEEE INFOCOM'98*, volume 2, pages 548–555, San Francisco, CA, Mar. 1998.

[11] A. E. Gamal, C. Nair, B. Prabhakar, E. U. Biyikoglu, and S. Zahedi. Energy-Efficient Scheduling of Packet Transmissions over Wireless Networks. In *Proc. IEEE INFOCOM'02*, volume 3, pages 1773–1782, New York City, NY, Jun. 2002.

[12] J. Gomez, A. T. Campbell, M. Naghshineh, and C. Bisdikian. Conserving Transmission Power in Wireless Ad Hoc Networks. In *Proc. IEEE ICNP'01*, pages 24–34, Nov. 2001.

[13] S. D. Gray and V. Vadde. Throughput and Loss Packet Performance of DCF with Variable Transmit Power. IEEE 802.11-01/227, May 2001.

[14] IEEE 802.11. *Part 11: Wireless LAN Medium Access Control (MAC) and Physical Layer (PHY) Specifications*. IEEE, Aug. 1999.

[15] IEEE 802.11a. *Part 11: Wireless LAN Medium Access Control (MAC) and Physical Layer (PHY) Specifications: High-speed Physical Layer in the 5 GHz Band*. Supplement to IEEE 802.11 Standard, Sep. 1999.

[16] IEEE 802.11b. *Part 11: Wireless LAN Medium Access Control (MAC) and Physical Layer (PHY) Specifications: High-speed Physical Layer Extension in the 2.4 GHz Band*. Supplement to IEEE 802.11 Standard, Sep. 1999.

[17] IEEE 802.11h/D2.2. *Part 11: Wireless LAN Medium Access Control (MAC) and Physical Layer (PHY) Specifications: Spectrum and Transmit Power Management extensions in the 5 GHz band in Europe*. Draft Supplement to IEEE 802.11 Standard-1999 Edition, Draft 2.2, Sep. 2002.

[18] Intersil Americas Inc. *2.4 GHz Power Amplifier and Detector*, Mar. 2000.

[19] Intersil Americas Inc. *Prism II 11Mbps Wireless Local Area Network PC Card*, Apr. 2001.

[20] E.-S. Jung and N. H. Vaidya. An Energy Efficient MAC Protocol for Wireless LANs. In *Proc. IEEE INFOCOM'02*, volume 3, pages 1756–1764, New York City, NY, Jun. 2002.

[21] P. Lettieri, C. Fragouli, and M. B. Srivastava. Low Power Error Control for Wireless Links. In *Proc. ACM MobiCom'97*, pages 139–150, Budapest, Hungary, 1997.

[22] B. O'Hara and A. Petrick. *The IEEE 802.11 Handbook: A Designer's Companion*. Standards Information Network, IEEE Press, 1999.

[23] B. Prabhakar, E. U. Biyikoglu, and A. E. Gamal. Energy-Efficient Transmission over a Wireless Link via Lazy Packet Scheduling. In *Proc. IEEE INFOCOM'01*, volume 1, pages 386–394, Anchorage, AK, Apr. 2001.

[24] D. Qiao and S. Choi. Goodput Enhancement of IEEE 802.11a Wireless LAN via Link Adaptation. In *Proc. IEEE ICC'01*, Helsinki, Finland, Jun. 2001.

[25] D. Qiao, S. Choi, A. Jain, and K. G. Shin. Adaptive Transmit Power Control in IEEE 802.11a Wireless LANs. In *Proc. IEEE VTC'03-Spring*, Jeju, Korea, Apr. 2003.

[26] D. Qiao, S. Choi, A. Soomro, and K. G. Shin. Energy-Efficient PCF Operation of IEEE 802.11a Wireless LAN. In *Proc. IEEE INFOCOM'02*, volume 2, pages 580–589, New York City, NY, Jun. 2002.

[27] T. S. Rappaport. *Wireless Communications: Principle and Practice*. Englewood Cliffs, NJ: Prentice-Hall, 1996.

[28] M. Rofougaran, A. Rofougaran, C. Olgaard, and A. A. Abidi. A 900 MHz CMOS RF Power Amplifier with Programmable Output. In *1994 Symposium on VLSI Circuits Digest of Technical Papers*, pages 133–134, Jun. 1994.

[29] J. F. Sevic. Statistical Characterization of RF Power Amplifier Efficiency for CDMA Wireless Communication Systems. In *Proc. Wireless Communications Conference*, pages 110–113, Boulder, CO, Aug. 1997.

[30] T. Simunic, L. Benini, P. Glynn, and G. D. Micheli. Dynamic Power Management for Portable Systems. In *Proc. ACM MobiCom'00*, pages 11–19, Boston, MA, Aug. 2000.

[31] M. Stemm, P. Gauthier, D. Harada, and R. H. Katz. Reducing Power Consumption of Network Interfaces in Hand-Held Devices. In *Proc. 3rd International Workshop on Mobile Multimedia Communications*, Princeton, NJ, Sep. 1996.

[32] H. Wang and P. Chang. On Verifying the First-Order Markovian Assumption for a Rayleigh Fading Channel Model. *IEEE Transactions on Vehicular Technology*, 45:353–357, May 1996.

[33] H. Wu, Y. Peng, K. Long, S. Cheng, and J. Ma. Performance of Reliable Transport Protocol over IEEE 802.11 Wireless LAN: Analysis and Enhancement. In *Proc. IEEE INFOCOM'02*, volume 2, pages 599–607, New York City, NY, Jun. 2002.

[34] K. Xu, M. Gerla, and S. Bae. How Effective is the IEEE 802.11 RTS/CTS Handshake in Ad Hoc Network. In *Proc. IEEE GlobeCom'02*, Taipei, Taiwan, Nov. 2002.

[35] M. Zorzi, R. R. Rao, and L. B. Milstein. Error Statistics in Data Transmission over Fading Channels. *IEEE Transactions on Communications*, 46(11):1468–1477, Nov. 1998.